From Armchair to Zigzag Peripheries in Nanographenes

Marcel Kastler, Jochen Schmidt, Wojciech Pisula, Daniel Sebastiani, and
Klaus Müllen*

*Contribution from the Max-Planck-Institute for Polymer Research, Postfach 3148,
D-55021 Mainz, Germany*

Received March 24, 2006; E-mail: muellen@mpip-mainz.mpg.de

Abstract: Synthetic concepts toward the synthesis of large, not-fully benzenoid polycyclic aromatic hydrocarbons (PAHs), decorated with phase-forming and solubilizing *n*-dodecyl chains, are presented based on the intramolecular cyclodehydrogenation reaction of suitable oligophenylene precursors. The formal addition of successive C2 units into the armchair bays of the parent hexa-*peri*-hexabenzocoronene extends the aromatic system and leads to PAHs with a partial zigzag periphery. This variation of the nature of the periphery, symmetry, size, and shape has a distinct impact upon the electronic properties and the organization into columnar superstructures. Both computational and experimental UV/vis spectra, which are in good agreement, emphasize the dependence of the characteristic bands α, p, and β upon the overall size and symmetry of the PAHs. While the number and the substitution patterns of attached *n*-dodecyl chains do not influence the electronic properties, the thermal behavior and supramolecular organization are strongly influenced, which has been elucidated with differential scanning calorimetry (DSC) and 2D wide-angle X-ray diffractometry (2D-WAXS) on mechanically aligned samples. This study provides valuable insight into the future design of semiconducting materials based on extended PAHs.

Introduction

Polycyclic aromatic hydrocarbons (PAHs) constitute a large and diverse class of organic molecules.[1] The major natural source on earth for PAHs is crude oil, coal, and oil shale.[2] The spectroscopy of interstellar material even proved the abundance of large PAHs, which are in fact the largest, detected molecules in space.[3] Some PAHs are widespread environmental pollutants and relatively potent carcinogens.[4]

Clar proposed that the properties of PAHs could be best understood in terms of localization of the aromatic sextets present in the molecules.[5] Fully benzenoid PAHs can formally be drawn only with Kekulé rings without isolated "double" bonds and are known to be kinetically very stable, unreactive substances. Two important examples of that class of compounds are triphenylene[6] and hexa-*peri*-hexabenzocoronene (HBC).[7] When substituted appropriately, many PAHs form very stable

columnar mesophases.[8] The intermolecular π-contact allows charge carrier migration[9] between the stacked discotic molecules, which opens the possibility to implement these structures in organic electronics, such as field-effect transistors, hole-injecting layers, or photovoltaic devices.[7,10] Recently, we presented a concept to synthesize a series of large, all-benzenoid PAHs with a broad range of sizes and shapes.[11]

Tetracene, a constitutional isomer of triphenylene, differs distinctly in its properties: lower resonance energy,[12] a lower ionization potential,[13] a smaller HOMO−LUMO gap,[13] and thermally far less stability.[5] This emphasizes inter alia the dependence of properties upon the nature of the periphery, symmetry, and shape.[14] Dias[15] discussed different perimeters for PAHs, where the two most prominent, zigzag and armchair edge, are shown in Figure 1.

Graphite and many carbonaceous materials consist primarily of large polyaromatic molecules of varying size, shape, and periphery. An understanding of the chemistry of graphite and

(1) (a) Scott, L. T.; Boorum, M. M.; McMahon, B. J.; Hagen, S.; Mack, J.; Blank, J.; Wegner, H.; de Meijere, A. *Science* **2002**, *295*, 1500−1503. (b) Harvey, R. G. *Curr. Org. Chem.* **2004**, *8*, 303−323. (c) Xiao, S. X.; Myers, M.; Miao, Q.; Sanaur, S.; Pang, K. L.; Steigerwald, M. L.; Nuckolls, C. *Angew. Chem., Int. Ed.* **2005**, *44*, 7390−7394.
(2) (a) Lehmann, E.; Auffarth, J.; Hager, J.; Rentel, K. H.; Altenburg, H. *Staub Reinhalt Luft* **1986**, *46*, 128−131. (b) Strewe, K.; Neumann, H. J. *Erdol Kohle Erdgas, Petrochem.* **1983**, *36*, 231−231. (c) Sullivan, R. F.; Boduszynski, M. M.; Fetzer, J. C. *Energy Fuels* **1989**, *3*, 603−612.
(3) (a) Duley, W. W.; Williams, D. A. *Mon. Not. R. Astron. Soc.* **1986**, *219*, 859−864. (b) Lovas, F. J.; McMahon, R. J.; Grabow, J. U.; Schnell, M.; Mack, J.; Scott, L. T.; Kuczkowski, R. L. *J. Am. Chem. Soc.* **2005**, *127*, 4345−4349.
(4) Harvey, R. G.; Dai, Q.; Ran, C. Z.; Lim, K.; Blair, I.; Penning, T. M. *Polycycl. Aromat. Compd.* **2005**, *25*, 371−391.
(5) Clar, E. *The Aromatic Sextett*; John Wiley & Sons: London, 1972.
(6) Adam, D.; Schuhmacher, P.; Simmerer, J.; Haussling, L.; Siemensmeyer, K.; Etzbach, K. H.; Ringsdorf, H.; Haarer, D. *Nature* **1994**, *371*, 141−143.
(7) Pisula, W.; Menon, A.; Stepputat, M.; Lieberwirth, I.; Kolb, U.; Tracz, A.; Sirringhaus, H.; Pakula, T.; Müllen, K. *Adv. Mater.* **2005**, *17*, 684−689.

(8) (a) de Halleux, V.; Calbert, J. P.; Brocorens, P.; Cornil, J.; Declercq, J. P.; Bredas, J. L.; Geerts, Y. *Adv. Funct. Mater.* **2004**, *14*, 649−659. (b) Wasserfallen, D.; Kastler, M.; Pisula, W.; Hofer, W. A.; Fogel, Y.; Wang, Z. H.; Müllen, K. *J. Am. Chem. Soc.* **2006**, *128*, 1334−1339. (c) Kastler, M.; Pisula, W.; Wasserfallen, D.; Pakula, T.; Müllen, K. *J. Am. Chem. Soc.* **2005**, *127*, 4286−4296. (d) Zimmermann, S.; Wendorff, J. H.; Weder, C. *Chem. Mater.* **2002**, *14*, 2218−2223.
(9) (a) van de Craats, A. M.; Warman, J. M.; Fechtenkötter, A.; Brand, J. D.; Harbison, M. A.; Müllen, K. *Adv. Mater.* **1999**, *11*, 1469−1472. (b) Meijer, E. W.; Schenning, A. *Nature* **2002**, *419*, 353−354.
(10) Schmidt-Mende, L.; Fechtenkötter, A.; Müllen, K.; Moons, E.; Friend, R. H.; MacKenzie, J. D. *Science* **2001**, *293*, 1119−1122.
(11) Müller, M.; Kübel, C.; Morgenroth, F.; Iyer, V. S.; Müllen, K. *Carbon* **1998**, *36*, 827−831.
(12) Hess, B. A.; Schaad, L. J. *J. Am. Chem. Soc.* **1971**, *93*, 305−310.
(13) Biermann, D.; Schmidt, W. *J. Am. Chem. Soc.* **1980**, *102*, 3173−3181.
(14) Dias, J. R. *Polycycl. Aromat. Compd.* **2005**, *25*, 113−127.
(15) Dias, J. R. *J. Chem. Inf. Comput. Sci.* **2005**, *45*, 562−571.

Scheme 1. Synthesis of the Asymmetrically Substituted HBC **1b**[a]

[a] (i) 93%; (ii) FeCl$_3$, 93%.

acene- or zigzag edge

phenanthrene type or arm-chair edge
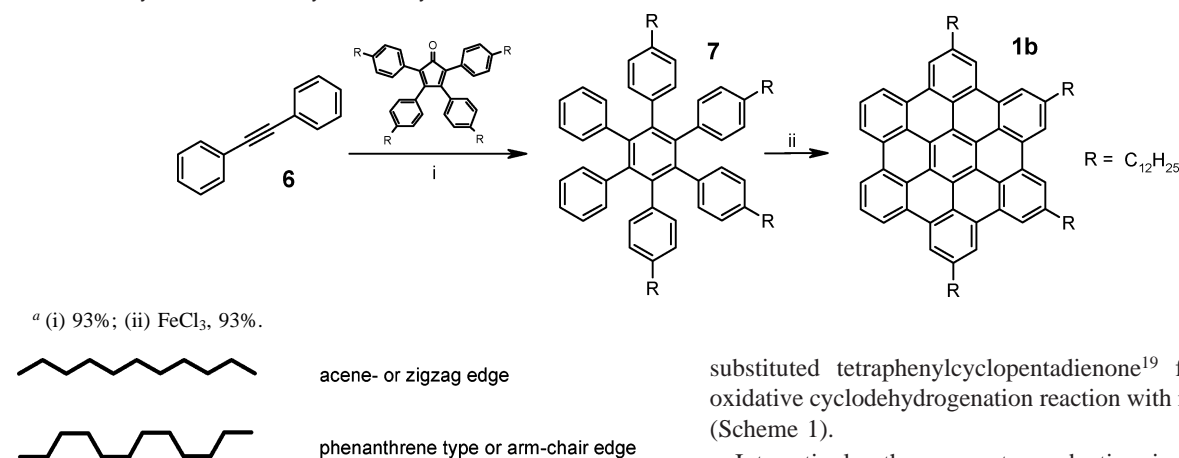
Figure 1. Different edge types for PAHs.

its physical properties is hampered by the inability to isolate the molecules for an individual study. Extended PAHs with different peripheries are required to test theoretical modeling of the properties of graphite.[16]

In this paper, we present novel synthetic concepts toward not fully benzenoid, phase-forming, extended PAHs. The formal introduction of C2 units into the armchair sites of the parent HBC led to a homologous series of four novel PAHs with varying symmetries, one composed of 44, two which contain 46, and finally, one which includes 48 carbon atoms within the aromatic moiety. All these extended PAHs, which contain zigzag sites, were substituted with multiple *n*-dodecyl chains on the perimeter to enhance the solubility and to generate a discotic liquid-crystalline phase behavior, which has been investigated using differential scanning calorimetry (DSC) and 2D wide-angle X-ray scattering (2D WAXS) of mechanically aligned fibers. The experimental and simulated UV/vis spectra, and the nature of the supramolecular organization for the novel materials with partial zigzag perimeter, were compared with the ones of different *n*-dodecyl-substituted hexa-*peri*-hexabenzocoronene, which contain only armchair sites, to explore the influence of the PAH symmetry, size, and periphery on these properties. These structural parameters of the molecules allowed a sensitive tuning of electronic properties, which is an important prerequisite for the successful implementation as semiconducting, active material in electronic devices.

Results and Discussion

Synthesis. The hexa-*n*-dodecyl-substituted HBC (**1a**) with D_{6h} symmetry has been synthesized according to the literature.[17] Another differently substituted HBC derivative has been prepared, which carried only four *n*-dodecyl chains in the corona of the aromatic disk.[18]

This 2,5,8,11-tetra-*n*-dodecyl-hexa-*peri*-hexabenzocoronene (**1b**) has been made in two steps via a Diels−Alder cycloaddition reaction between diphenylacetylene and the *n*-dodecyl-substituted tetraphenylcyclopentadienone[19] followed by an oxidative cyclodehydrogenation reaction with iron(III) chloride (Scheme 1).

Interestingly, the symmetry reduction in the substitution pattern of **1b** enhanced the solubility significantly compared to that of **1a**, although fewer solubilizing chains were attached. Both **1a** and **1b** contain only armchair sites and will be used as reference compounds. In the following, the synthesis of PAHs with a partial zigzag periphery will be presented.

The synthesis of the 44 aromatic carbons containing PAH **2** with one zigzag site started with 4-methoxyphenanthrene (**8**), which has been synthesized by transition-metal-catalyzed cycloisomerization according to Fürstner's protocol (Scheme 2).[20] Demethylation with boron tribromide yielded the corresponding alcohol, which was converted into the nonaflate derivative **9** in good yields. Compound **9** proved to be more reactive in the Hagihara-Sonogashira cross-coupling than the tosylate or the triflate and led to the trimethylsilyl-protected acetylene derivative. After desilylation, the Diels−Alder conversion of the 4-ethynylphenanthrene (**10**) with alkyl-substituted tetraphenyl-cyclopentadienone afforded the precursor **11** in excellent yields. High field NMR spectroscopy permitted resolution of all proton resonances for **11**, which could be assigned utilizing H,H COSY and NOESY experiments (Supporting Information). The line broadening of the phenyl proton signals at room temperature suggested that the phenyl group rotation was slow on the NMR time scale. Finally, **11** was oxidatively planarized with iron-(III) chloride to the 8,11,14,17-tetra-*n*-dodecyl-tetrabenzo[bc,-ef,hi,uv]ovalene (**2**) in good yields.

For the synthesis of the PAH **3** with 46 aromatic carbon atoms and two zigzag edges, pyrenediketone **12**[21] was converted in a double Aldol condensation with 1,3-bis(4-bromophenyl)-2-propanone[22] to the thermally unstable cyclopentadienone derivative **13**, which precipitated during the reaction (Scheme 3). The analogous condensation with the *n*-dodecyl-substituted 1,3-diphenyl-propan-2-one led only to traces of the desired product because it decomposed already during the reaction due to its good solubility in ethanol. Despite the thermal instability, in the presence of **10**, **13** underwent at higher temperatures a Diels−Alder reaction, affording the PAH **14**. Hydroboration of dodecene with 9-BBN and subsequent Suzuki cross-coupling reaction with the bromo-functions in **14** afforded the bis-alkylated derivative **15** in good yields. In contrast to the

(16) (a) Stein, S. E.; Brown, R. L. *J. Am. Chem. Soc.* **1987**, *109*, 3721−3729. (b) Nakada, K.; Fujita, M.; Dresselhaus, G.; Dresselhaus, M. S. *Phys. Rev. B* **1996**, *54*, 17954−1796. (c) Takagi, Y.; Fujita, M.; Igami, M.; Kusakabe, K.; Wakabayashi, K.; Nakada, K. *Synth. Met.* **1999**, *103*, 2574−2575.
(17) Herwig, P.; Kayser, C. W.; Müllen, K.; Spiess, H. W. *Adv. Mater.* **1996**, *8*, 510−513.
(18) Pisula, W.; Tomovic, Z.; Simpson, C.; Kastler, M.; Pakula, T.; Müllen, K. *Chem. Mater.* **2005**, *17*, 4296−4303.
(19) Iyer, V. S.; Yoshimura, K.; Enkelmann, V.; Epsch, R.; Rabe, J. P.; Müllen, K. *Angew. Chem., Int. Ed. Engl.* **1998**, *37*, 2696−2699.
(20) Fürstner, A.; Mamane, V. *J. Org. Chem.* **2002**, *67*, 6264−6267.
(21) Young, E. R. R.; Funk, R. L. *J. Org. Chem.* **1998**, *63*, 9995−9996.
(22) Ito, S.; Wehmeier, M.; Brand, J. D.; Kübel, C.; Epsch, R.; Rabe, J. P.; Müllen, K. *Chem. Eur. J.* **2000**, *6*, 4327−4342.

Scheme 2. Synthesis of PAH **2** with One Zigzag Site[a]
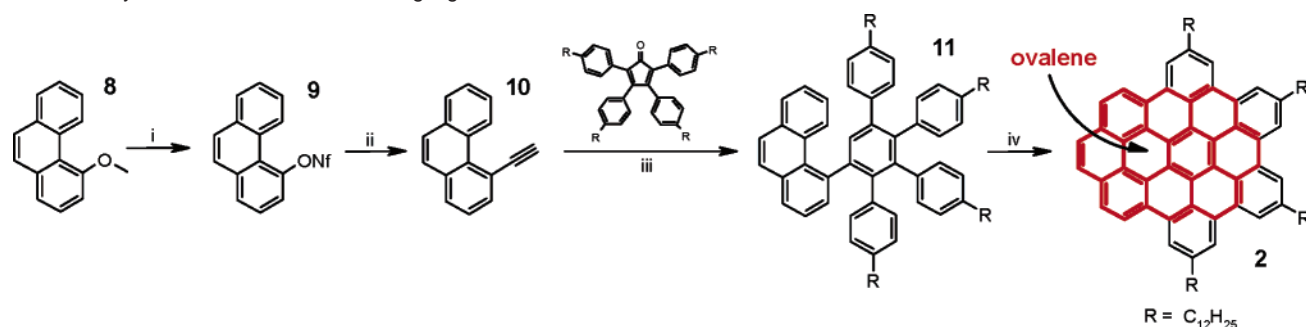
[a] (i) BBr$_3$, 86%; NfF, NEt$_3$, 93%; (ii) trimethylsilylacetylene, CuI, PPh$_3$, Cl$_2$Pd(PPh$_3$)$_3$, 87%; K$_2$CO$_3$, MeOH, 95%; (iii) 95%; (iv) FeCl$_3$, 79%. The ovalene moiety is colored in red in structure **2** to better comprehend the IUPAC nomenclature.

Scheme 3. Synthesis of PAH 2 with Two Zig-zag Sites[a]
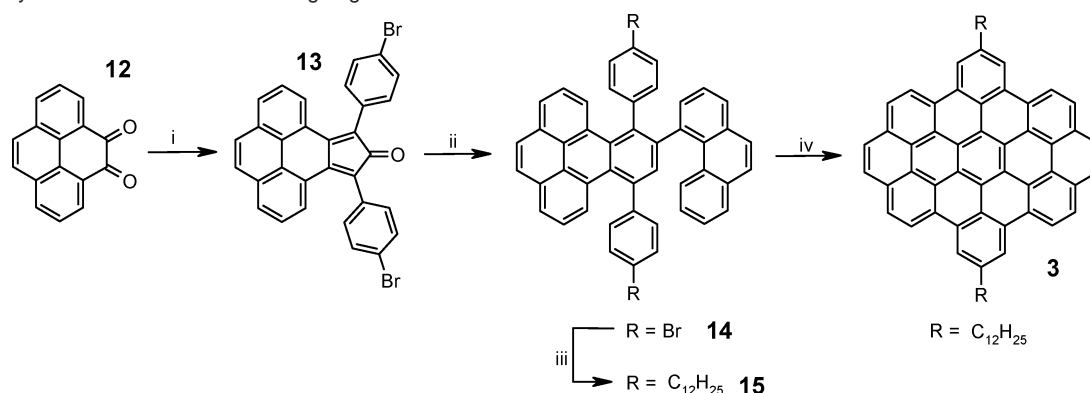
[a] (i) 1,3-Bis-(4-bromo-phenyl)-propan-2-one, KOH, 47%; (ii) 75%; (iii) dodeca-1-ene, 9-BBN, KOH, Cl$_2$Pd(dppf), 91%; (iv) FeCl$_3$, 90%.
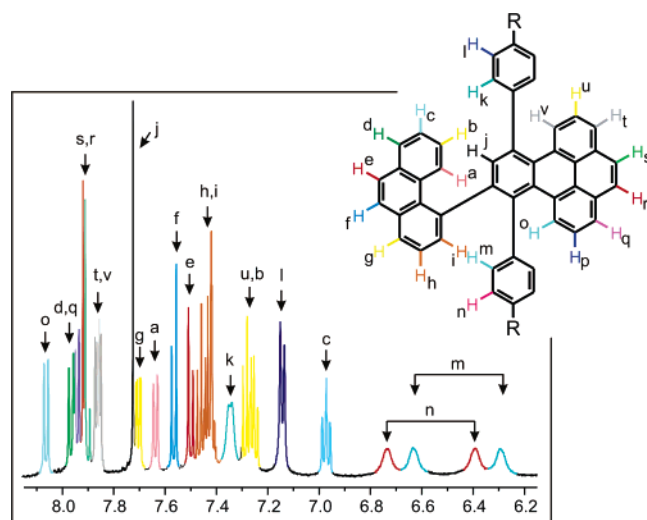

Figure 2. Aromatic region of the ^{1}H NMR spectrum of **15**, recorded in 1,1,2,2-tetrachloroethane-d_2 at 100 °C (500 MHz).

precursor **11**, the rotation of the phenyl with the protons *m* and *n* was even at elevated temperatures (<180 °C) slow on the time scale of the NMR experiment (Figure 2), leading to four broad resonances.

Analogous to **11**, all proton resonances could be assigned using H,H COSY and NOESY experiments on a high-field instrument. Finally, 8,17-bis-*n*-dodecyl-dibenzo[hi,uv]phenan-thro-(3,4,5,6-bcdef)-ovalene (**3**) was obtained after the successful oxidative cyclodehydrogenation. Although hardly soluble, it was possible to obtain a resolved ^{1}H NMR spectrum of the PAH **3** (Supporting Information).

For both the 44 and 46 aromatic carbon atoms containing PAHs **4** and **5**, which include two and three zigzag sites, respectively, 4-methoxy-phenanthrene-9,10-dione (**16**) was synthesized in good yield following the published procedure.[23] The reaction of the carbonyl centers with *n*-dodecylmagnesium bromide led to the corresponding diol which was reduced with iodic acid directly to the 9,10-dialkylated phenanthrene (Scheme 4). At the same time, the reaction conditions allowed demethyl-ating the methoxy function. The separation of the desired phenanthrenol from side products turned out to be difficult, so the crude compound was converted with nonafluoro-butane-1-sulfonyl fluoride to the nonaflate **17**, which could be easily purified. Optimized conditions allowed the conversion of **17** to the pinacol boronic ester **18** in good yields using tetrakis-(triphenylphosphino)palladium(0) as catalyst in DMF. The Suzuki cross-coupling reaction with 1,3,5-tribromobenzene required a strong base to yield the sterically crowded precursor molecule **21**. Temperature-dependent ^{1}H NMR experiments proved that the molecule existed as two stable atropisomers (Supporting Informaiton) in solution at room temperature, and temperatures of about 180 °C were needed to promote the free rotation of the phenanthrenyl units around the central benzene ring (Supporting Information). The oxidative cyclodehydroge-nation reaction of **21** with iron(III) chloride produced the fully planarized PAH, 5,6,11,12,17,18-hexa-*n*-dodecyl-diphenanthro-[3,4,5,6-uvabc;3′,4′,5′,6′-efghi]ovale ne (**5**), in high yield.

The Suzuki cross-coupling reaction of **18** with 1,3,5-tribro-mobenzene gave as a major product the less crowded compound **19**, which was isolated and subsequently coupled with com-

(23) Cai, X. W.; Brown, S.; Hodson, P.; Snieckus, V. *Can. J. Chem.* **2004**, *82*, 195−205.

Scheme 4. Synthesis of PAHs **4** and **5** with Two and Three Zigzag Sites[a]

R = $C_{12}H_{25}$
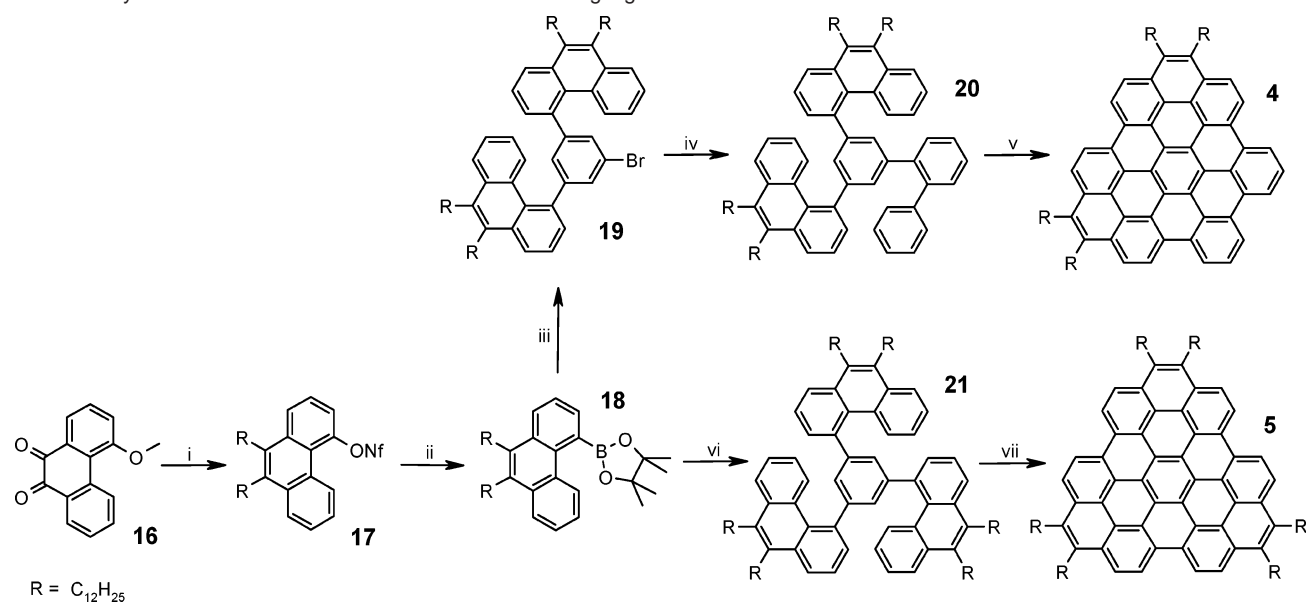
[a] (i) RMgBr; HI, AcOH; NfF, NEt₃, 90%; (ii) bispinacolatodiborane, AcOK, Pd(PPh₃)₄, 72%; (iii) 1,3,5-tribromobenzene, Ba(OH)₂, Pd(PPh₃)₄, 70%; (iv) 2-biphenylboronic acid, Ba(OH)₂, Pd(PPh₃)₄, 71%; (v) FeCl₃, 91%; (vi) 1,3,5-tribromobenzene, Ba(OH)₂, Pd(PPh₃)₄, 8%; (vii) FeCl₃, 83%.
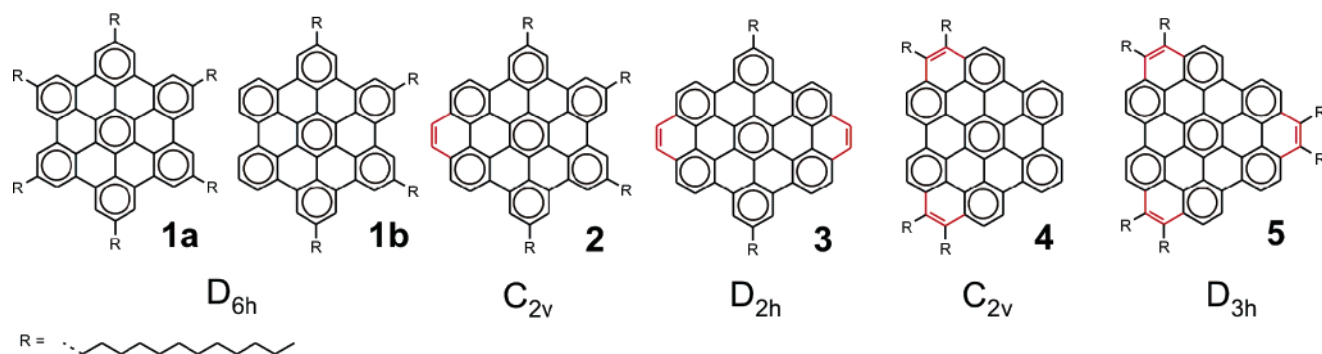
Figure 3. Investigated PAHs written in the Clar nomenclature including the symmetry group of the aromatic core.

mercially available 2-biphenylboronic acid to obtain the precursor **20**. Interestingly, the reaction was high yielding and the compound did not form stable atropisomers because the more flexible biphenyl unit could not hinder the rotation of the phenanthrenyl units at room temperature on the time scale of the NMR. After the planarization reaction, the PAH, 5,6,17,-18-tetra-*n*-dodecyldibenzo[ef,hi]phenanthro[3,4,5,6-u,v,a,b,c]-ovalene (**4**), could be isolated in high yield.

The previously described oxidation[24] of the zigzag sites in the PAHs **3**–**5** toward their corresponding *o*-quinone analogues was attempted but in these cases no desired product could be identified by mass spectrometry. Contrary to **2**, where the electron density was polarized toward the zigzag site, the localization of charge was less pronounced in PAHs with multiple zigzags, which has been supported by calculations (Supporting Information).

The above syntheses of four novel, extended, soluble nanographenes with different peripheries (Figure 3) and symmetry points groups afford unprecedented model systems for graphite. In the following, their properties will be investigated by electronic spectroscopy and their propensity to pack into columnar superstructures will be elucidated by 2D-WAXS experiments.

Spectroscopy. Typically, PAHs reveal three bands with increasing intensity. Clar[25] introduced the nomenclature α-, p-, and β-band, which originated from empirically determined correlation between the so-called "ortho" and "para" reactivity and the absorption spectra. The weak α-band appears usually at the highest wavelength of the three and corresponds to a transition from the second highest occupied molecular orbital (HOMO−1) to the lowest unoccupied molecular orbital (LUMO).[26] This is also known as the 0−0 transition. The very intense β-band possesses the lowest wavelength of the three and corresponds to a transition from the highest occupied molecular orbital (HOMO) to the second lowest unoccupied orbital (LUMO+1).[26] The p-band is of intermediate wavelength and intensity and can be assigned to a transition from HOMO to LUMO.[26] However, in the case of symmetric molecules, this transition can be symmetry forbidden, which is independent of the normal dipole selection rules.[27]

The number and the oscillator strength of the transitions in the usually structure-rich absorption spectra are mainly dependent on the symmetry and the topology of the molecule.[5,25,28] The characteristic absorption and photoluminescence (PL) spectra

(24) Wang, Z. H.; Tomovic, E.; Kastler, M.; Pretsch, R.; Negri, F.; Enkelmann, V.; Müllen, K. *J. Am. Chem. Soc.* **2004**, *126*, 7794−7795.

(25) Clar, E. *Polycyclic Hydrocarbons*; Academic Press and Springer-Verlag: London, 1964; Vols. I+II.

(26) Fetzer, J. C. *Large (C>=24) Polycyclic Aromatic Hydrocarbons*; John Wiley & Sons: New York, 2000.

Table 1. Comparison between the Calculated Excitation Energies (*E*) and Oscillator Strengths (*f*) and the Experimentally Determined Energies of the PAHs **1**−**5**

	transition	*E* (eV) exp.	*E* (eV) calc.	*f* (calc)
1	a	2.66	2.90	0.00
	p	3.16	3.03[a]	0.00
	b	3.42	3.48	0.72
2	a	2.56	2.75	0.0001
	p	2.62	2.79[b]	0.15
	b	3.26	3.26	0.31
3	a	2.43	2.72	0.0003
	p	2.62	2.62[c]	0.26
	b	3.12	3.21	0.71
4	a	2.53	2.66	0.0003
	p	2.77	2.64[d]	0.18
	b	3.20	3.26	0.02
5	a	2.33	2.55	0.00
	p	2.92	2.67[e]	0.00
	b	3.11	3.20	0.91

[a] Wave function composition: −0.49 (H−1 → L+1), 0.49 (H → L). [b] Wave function composition: 0.27 (H−1 → L+1), 0.11 (H−1 → L+2), 0.62 (H → L). [c] Wave function composition: −0.23 (H−1 → L+1), 0.63 (H → L). [d] Wave function composition: −0.23 (H−1 → L+1), 0.64 (H → L). [e] Wave function composition: 0.50 (H−1 → L+1), 0.50 (H → L).

of the novel PAHs **2**−**5** (Figure 3) will now be compared with those of the parent compound **1a** (Figure 4). The observations are summarized in the following:

(i) The electronic spectra of **1b**, with a different substitution pattern, were identical with that of **1a**. This emphasizes that the alkyl substituents have no effect upon the electronic spectroscopy.

(ii) The PAHs with a higher symmetry group such as **1** (D_{6h}) or **5** (D_{3h}) exhibit narrow UV/vis spectra, with only few transitions and broader PL spectra compared to their lower symmetric counterparts **2**−**4**. Furthermore, the energy space between the absorption and the PL bands is larger for PAHs with a higher symmetry group.

(iii) Symmetry reduction led to more allowed transitions and therefore to broader, less structured UV/vis absorption spectra in the case of the C_{2v}-symmetric PAHs **2** and **4**. Even the usually weak α-bands were more intense.
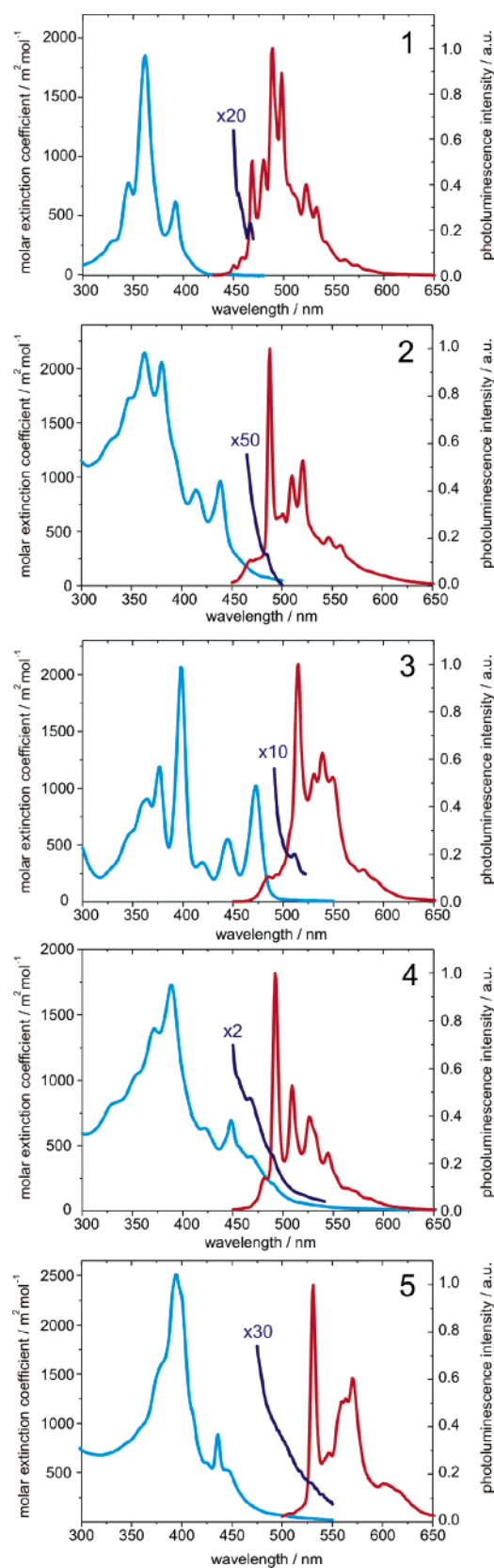
(iv) The PL spectra of the PAHs **1**−**5** revealed many sharp bands, which is typical for a symmetry-forbidden transition from the S_1 to the ground state S_0. Therefore, different vibronic levels of the ground state were reached from the excited state, leading to a set of distinct peaks.

(v) The 0−0 transition in the PL spectrum for the D_{6h} symmetric PAH **1** is only weakly allowed, while it becomes the strongest band when the symmetry was reduced.

(vi) The molar extinction coefficients of the most intense UV/vis absorption band for the PAHs **1**−**5** were in the same range.

(vii) The Stokes shift was in all cases very small (<5 nm) and independent of the solvent used, which indicated no polarity difference of the ground and the excited state which has been observed for other PAHs as well.[8b]

Quantum chemical calculations were carried out to determine energies and intensities of the excitations, using a density functional theory (DFT) approach. The structures of PAHs **1**−**5** were first optimized on the B3LYP/3-21G level and subse-

(27) (a) Zander, M. *Fluorimetrie*; Springer-Verlag: Berlin, 1981. (b) Becker, R. *Theory and Interpretation of Fluorescence and Phosphorescence*; Wiley-Interscience: New York, 1969.
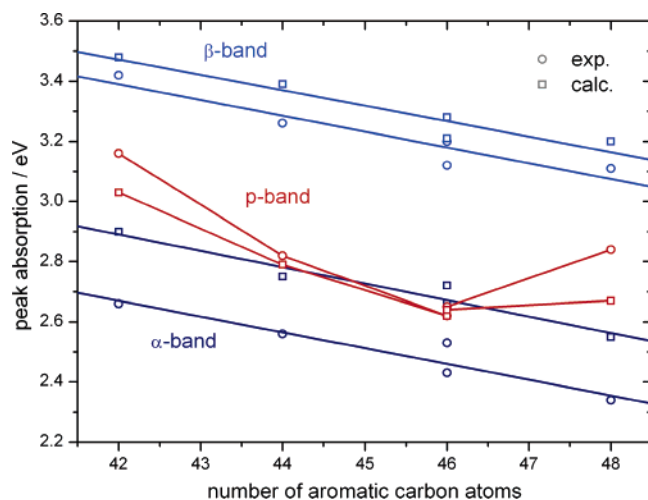(28) Harvey, R. G. *Polycyclic Aromatic Hydrocarbons*; Wiley-VCH: New York, 1997.

Figure 4. UV/vis and photoluminescence emission spectra of PAHs **1**−**5**; the α-bands are magnified for better visualization.

quently a TDDFT (time-dependent DFT)[29] calculation (B3LYP/6-31G(d)) was conducted. The calculations are in good agreement with the experimentally determined peak positions (Table 1), and the error is within the expected range for this type of

Figure 5. Dependence of the absorption bands from the size of the aromatic core for **1−5**.

compound, as shown in calculations for various polycyclic aromatic hydrocarbons.[30]

With increasing size of the aromatic system, we expect a smaller band gap and thus decreasing excitation energies. Plotting the absorption maximum of the α- and the β-band, respectively, versus the number of carbon atoms in the aromatic system, one finds both for the experimental and the calculated data a linear dependence (Figure 5). The energy of these transitions exhibits only a dependence upon the size of the aromatic system and is thus not influenced by the nature of the periphery or the symmetry of the aromatic system.

In contrast, the p-band, which originally corresponds to the transition between the HOMO and the LUMO,[26] does not reveal a simple linear dependence upon the size of the aromatic system. The calculation revealed that this band not only is due to a HOMO−LUMO transition but also involves the transition between HOMO−1 and LUMO+1 (Table 1). In the case of PAH **2** there is even a small contribution of HOMO−1 to LUMO+2. The nonlinear behavior of the p-band can be understood qualitatively by the ordering of the orbital energies. Figure 6 shows the energy of the orbitals HOMO − 1, HOMO, LUMO, and LUMO + 1 taken from a ground-state calculation.
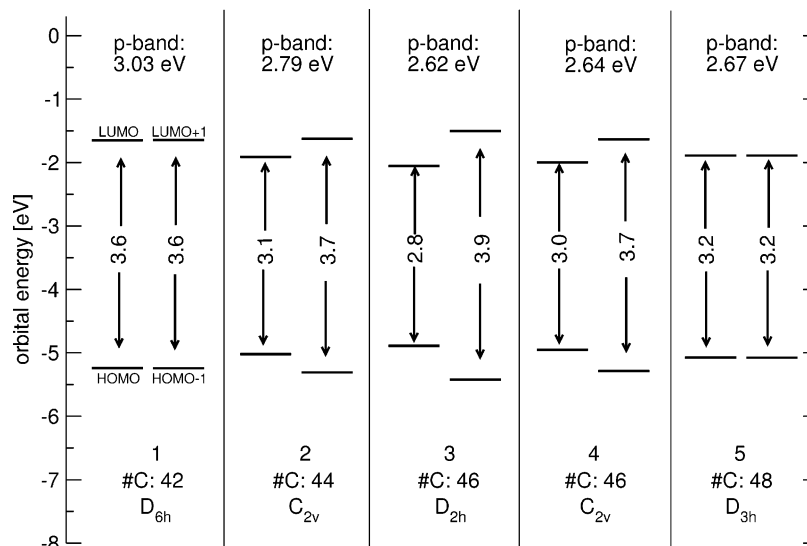
The PAHs **1** and **5** are the most symmetrical ones (D_{6h} and D_{3h}), leading to degeneracy of HOMO/HOMO−1 and LUMO/LUMO+1. The resulting band gap is larger than the ones of the less symmetrical molecules. In the case of the PAHs **2−4** the HOMO−LUMO transition gives the largest contribution to the p-band (see the corresponding coefficients in Table 1) and thus the excitation energy is smaller. The oscillator strengths, as a measure for the intensity of the bands, indicate that the p-band in the symmetrical cases (PAH **1** and **5**) is symmetry-forbidden. These results agree with group theoretical examinations of the ground and excited states.[31] Despite this, the corresponding line appears in the experimental spectrum because at finite temperatures the symmetry is dynamically broken and the strict selection rule does not hold anymore. As indicated in Figure 6, the excitation energy of the p-band taken from the TDDFT calculation does not correspond to the HOMO−LUMO gap as computed in the electronic ground state. This is a well-known phenomenon which is due to the interaction of the excited electron with the remaining valence electrons. However, since this is a perturbative effect, the ordering of the energies is preserved in general and thus the above discussion still holds.

For all investigated PAHs, the ratio between the peak wavelength of the α- and the β-band was constant, which has been empirically reported already by Clar[25] for substantially smaller compounds.

Supramolecular Organization. The substitution of the aromatic systems with flexible alkyl chains enhanced on one hand the solubility to obtain a material which could be characterized by solution analytics. On the other hand, the flexible substituents imposed on the rigid aromatic cores in many cases a discotic phase behavior. In the past, discotic materials have gained great importance as promising, active components in organic devices.[6,32] Compound **1a** was successfully implemented in field-effect transistors,[7,33] while other derivatives served as donor component in organic heterojunction photovoltaic devices.[10] In these applications, long-range and defect-free organizations of the planar, aromatic molecules are required to yield high-performance values in the electronic device.

In the following, the thermal behavior and supramolecular organization of the novel, liquid-crystalline PAHs **1−5** (Figure

Figure 6. Orbital energies in the ground state of the PAHs **1−5**. Also given are the excitation energy of the p-band from the TDDFT calculation, the number of the aromatic carbon atoms, and the symmetry group of the molecule.

Table 2. Phase Behavior of the PAHs **1**−**5**[a]

derivative	temperature (°C)	enthalpy (J g⁻¹) (1st transition during heating)	phase transition
1a	107 (82)	45.8	$C_r - Col_{ho}$
	420*		$Col_{ho} - I$
1b	147 (123)	15.7	$C_r - Col_{ho}$
	400*		$Col_{ho} - I$
2	148 (98)	13.8	$C_r - Col_{ho}$
	400*		$Col_{ho} - I$
3	226 (216)	28.3	$C_r - ?$
	>500*		$Col_{ho} - I$
4	173 (144)	11.5	$C_r - Col_{co}$
	210		$Col_{co} - I$
5	48 (22)	18.4	$C_r - Col_{ho}$
	>500*		$Col_{ho} - I$

[a] List of abbreviations: C_r, crystalline phase; Col_{ho}, mesophase (hexagonal ordered columnar phase); Col_{co}, mesophase (cubic ordered columnar phase); I, isotropic phase. Phase transitions upon cooling are given in brackets. (*) Assigned by polarized optical microscopy.

3) will be described to gain a further understanding of how periphery, symmetry, and substitution pattern of the PAH influence the nature of the packing in the bulk.

Thermal Behavior. The thermal behavior, which is summarized in Table 2, was determined by differential scanning calorimetry (DSC) and polarized optical microscopy (POM). These data give insight into the stability of the respective phases and transition enthalpies dependent upon the molecular architecture, which can be correlated to the propensity of the molecules to establish the supramolecular organizations.

All investigated PAHs were crystalline-like at room temperature. The comparison of the thermal data showed a stronger dependence on the number and the substitution pattern of the *n*-dodecyl side chains than on the shape and symmetry of the aromatic core. Thus, with increasing number of alkyl chains the phase transition temperature from the crystalline phase to the mesophase decreased. Therefore, independent of the symmetry of the aromatic core, derivatives **1b**, **2**, and **4** entered the mesophase at significantly higher temperatures than **1a** and **5** with more alkyl side chains. Moreover, the density of substitution and consequently the steric hindrance played an additional effect, as was obvious for the D_{3h}-symmetric compound **5** which revealed the lowest first transition temperature. On the other hand, the DSC data suggested that a higher symmetry group of the aromatic core enhanced the intermolecular forces and thus affected the isotropization temperature, which is much higher for the symmetric PAHs **1a**, **3**, and **5** in comparison to the derivatives consisting of an asymmetric core like **4** melting already at 210 °C. The enthalpy of the phase transition (Table 2) is an indication for the change of the organization between two phases. Therefore, assuming a similar order in the mesophase for all derivatives, the enthalpy of the first phase transition increases with increasing crystallinity of the material and thus with higher supramolecular order in the crystalline

phase. This relation was in good agreement with the determined organization in the respective phases, as described in the next section.

Self-assembly. Both concentration- and temperature-dependent NMR spectroscopy and the electronic spectra from solution doubtless indicated a pronounced tendency of all investigated PAHs to self-assemble in solution. The analysis of the respective spectra revealed a similar association behavior which has already been previously observed for different HBC derivatives.[8c] For the investigation in the bulk phase, specimen for the 2D-WAXS experiments were prepared by filament extrusion as described previously.[18] All derivatives were extruded in their deformable, plastic state to ensure an adequate alignment of the columnar structures along the shear direction. For reasonable comparison of the supramolecular organization of all derivatives, the patterns were recorded at room temperature before annealing, which could influence strongly the molecular packing as observed for **1b**.[18] Temperature-dependent measurements gave additional insight into the order in the higher temperature phases. Except compound **4**, all derivatives revealed a characteristic hexagonal mesophase with a nontilted intracolumnar organization above the first transition. In contrast, the pronounced asymmetry of **4** resulted in a tilted packing of the disks toward the columnar axis and a cubic intercolumnar arrangement in the mesophase.

All derivatives, except **3**, arranged in a "herringbone" manner[34] with tilted molecules within the columns, whereby the tilting angle varied only slightly when derived from the azimuthal angle of the off-meridional reflections. The variation of the positions of the equatorial reflections implied differences of the lateral 2D unit cells, which were dependent on the size of the aromatic core and the number of *n*-dodecyl side chains. In general, the intensity and sharpness of the reflections were a strong indication of the degree of supramolecular order.

Figures 7 and 8 show the patterns for the higher symmetric compounds **1a**, **3**, and **5** and the "asymmetrical" derivatives **1b**, **2**, and **4**, respectively. It is obvious that the higher symmetric aromatic core enhanced the supramolecular order. The reflections indicating both the inter- and intracolumnar arrangement for the compounds possessing a higher symmetric design were sharper and more distinct in comparison to the ones for the less symmetric PAHs. The highest degree of crystallinity was observed for **3** due to the small number of only two *n*-dodecyl side chains and the relatively high D_{2h} core symmetry. The resulting structure gave rise to multiple meridional reflections with a nontilted intracolumnar arrangement, implying an extraordinary high intracolumnar order. Both symmetrical **1a** and **5** differed in the core size and the position of substitution of the six *n*-dodecyl chains. Since the pattern of **1a** revealed more distinct, higher order reflections, one could assume that in this case the slight core increase did not play any role in the organization of the molecules. However, the distribution of the alkyl side chains around the core influenced the packing to a greater extent.

In the case of **5**, the alkyl substituents are paired on two neighboring carbon atoms in the periphery of the PAH. This leads due to steric reasons to a worse packing than that of the HBC **1a**, where the substitution point of the *n*-dodecyl chains are well-distributed at the corona.

(29) Jamorski, C.; Casida, M. E.; Salahub, D. R. *J. Chem. Phys.* **1996**, *104*, 5134−5147.
(30) Parac, M.; Grimme, S. *Chem. Phys.* **2003**, *292*, 11−21.
(31) Bräuchle, C. *Chem. Phys.* **1982**, *67*, 97−109.
(32) Boden, N.; Bushby, R. J.; Clements, J.; Movaghar, B. *J. Mater. Chem.* **1999**, *9*, 2081−2086.
(33) van de Craats, A. M.; Stutzmann, N.; Bunk, O.; Nielsen, M. M.; Watson, M.; Müllen, K.; Chanzy, H. D.; Sirringhaus, H.; Friend, R. H. *Adv. Mater.* **2003**, *15*, 495−499.

(34) Fischbach, I.; Pakula, T.; Minkin, P.; Fechtenkötter, A.; Müllen, K.; Spiess, H. W.; Saalwächter, K. *J. Phys. Chem. B* **2002**, *106*, 6408−6418.
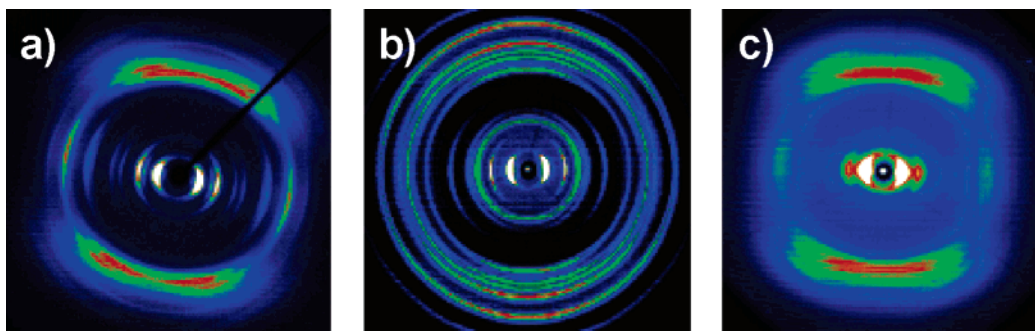
Figure 7. Room-temperature 2D-WAXS patterns of derivatives with a high-symmetry group (a) **1a**, (b) **3**, and (c) **5**.
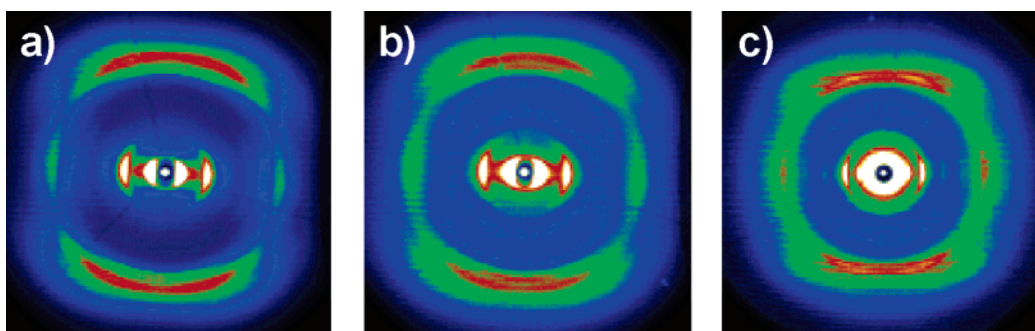

Figure 8. Room-temperature 2D-WAXS pattern of derivatives with lower symmetry group as (a) **1b**, (b) **2**, and (c) **4**.

The lower symmetry decreased additionally the supramolecular order as in the case of **1b**, **2**, and **4**. In all three 2D-WAXS patterns both equatorial and meridional reflections became more diffuse and weak. Especially compound **4**, consisting of a core with a low symmetry and a high number of directly "neighboring" substituents, revealed the highest degree of disorder. The equatorial first-order reflections, characteristic of the intercolumnar arrangement, were almost isotropic, suggesting a poor alignment of the columnar structures in the extruded samples. However, sharper off-meridional reflections might imply a more uniform tilting of the disks than in the other investigated cases. According to the thermal behavior of compounds **1b** and **2**, the additional two carbon atoms within the core also did not affect the molecular packing to a great extent. The 2D-WAXS results demonstrate clearly the influence of the symmetry of the aromatic core, the size of the aromatic system, and the substitution pattern upon the supramolecular organization. This emphasizes the importance of the molecular architecture on the formation of the supramolecular structures, which is important for the future syntheses of discotic materials for potential application in electronic devices.

Conclusion

The synthesis of a homologous series of extended, not-fully benzenoid PAHs, which differed in size and symmetry of their aromatic system, has been described. The synthetic routes toward these PAHs were all based on final oxidative cyclodehydrogenation reactions of precursors with adequate architectures, in which different smaller PAH moieties were introduced. The introduction of different phenanthrenyl units into the precursor molecules allowed the periphery of the final PAH to be successively modified from fully armchair to partially zigzag. This opened the possibility to investigate the role of symmetry, size, and periphery in molecular and supramolecular properties.

The synthetic concept allowed decoration of the rigid aromatic systems with multiple *n*-dodecyl side chains to guarantee solubility and liquid-crystalline phase behavior.

The change of the symmetry, which goes along with the partial change of the periphery type, had a pronounced influence upon the electronic spectra. Both the experimental and computational UV/vis spectra were in good agreement and revealed that the spectra of highly symmetric molecules were transition poor compared to the PAHs with lower symmetries. The PAH typical bands α and β depended linearly upon the overall size of the aromatic system, while the position of the p-band was mainly controlled by the symmetry of the PAH. The number and the substitution pattern of the *n*-alkyl chains did expectedly not have any influence upon these molecular properties. In contrast, the nature of the flexible surrounding on the PAH imposed its character onto the supramolecular organization of the synthesized mesogens. All investigated compounds exhibited a columnar mesophase, whereby the symmetry of the aromatic part influenced only the stability of the arrangement as measured by DSC. However, the number and the position of the flexible alkyl chains controlled both the thermal behavior and the quality of the supramolecular organization. Fewer chains with a symmetric arrangement around the aromatic disk caused a stabilization of the columnar organization due to an unperturbed aromatic π-stacking. More chains, which were asymmetrically distributed on the periphery of the PAH, were more difficult to pack, and hence the columnar arrangement exhibited more defects and a smaller long-range correlation. The enthalpy of the first transition in the DSC reflected the degree of crystallinity in the room temperature phase, which was directly related to the symmetry of the core and the substitution pattern. A pronounced higher order in the crystalline phase was thus found for the higher symmetry compounds, whereby the organization of the mesophase was comparable for all PAHs in the investigated homologous series.

The tuning of electronic properties and the control of the organization into long-range oriented molecular stacks are a challenge for materials science in a quest for novel, semiconducting materials with specific properties. The absorption behavior and the position of the molecular orbitals were two important parameters that influence the performance of organic heterojunction photovoltaic devices. It is known that a high supramolecular order enhances the charge carrier transport along the one-dimensional structures.[35] Therefore, the development of organic semiconductors which self-assemble into highly organized arrays is one major goal. The tuning of electronic levels of the active component in an electronic device is of key importance to reduce charge carrier injection barriers at the electrodes or to optimize the exciton polarization in solar cells.

This study elucidated the importance of the molecular design on the molecular properties and self-organization and gave important insights into the future development of semiconducting materials based on discotic PAHs.

Supporting Information Available: Experimental procedures, characterization for the described compounds, MALDI spectra, enlarged electronic spectra of the PAHs **2**−**5**, and additional computational data. This material is available free of charge via the Internet at http://pubs.acs.org. See any current masthead page for ordering information and Web access instructions.

JA062026H

(35) Paraschiv, I.; Giesbers, M.; van Lagen, B.; Grozema, F. C.; Abellon, R. D.; Siebbeles, L. D. A.; Marcelis, A. T. M.; Zuilhof, H.; Sudholter, E. J. R. *Chem. Mater.* **2006**, *18*, 968−974.